THE JOURNAL OF BIOLOGICAL CHEMISTRY VOL. 285, NO. 21, pp. 16378–16386, May 21, 2010

Reduction of Sympathetic Activity via Adrenal-targeted GRK2 Gene Deletion Attenuates Heart Failure Progression and Improves Cardiac Function after Myocardial Infarction*

Received for publication, October 21, 2009, and in revised form, March 8, 2010 Published, JBC Papers in Press, March 29, 2010, DOI 10.1074/jbc.M109.077859

Anastasios Lymperopoulos[‡§1], Giuseppe Rengo[§2], Erhe Gao[§], Steven N. Ebert[¶], Gerald W. Dorn II[‖], and Walter J. Koch[§]

From the [‡]Department of Pharmaceutical Sciences, Nova Southeastern University College of Pharmacy, Ft. Lauderdale, Florida 33328, the [§]Center for Translational Medicine and the George Zallie and Family Laboratory for Cardiovascular Gene Therapy, Department of Medicine, Thomas Jefferson University, Philadelphia, Pennsylvania 19107, the [¶]Burnett School of Biomedical Sciences, College of Medicine, University of Central Florida, Orlando, Florida 32827, and the [‖]Center for Pharmacogenomics, Department of Internal Medicine, Washington University, St. Louis, Missouri 63110

Chronic heart failure (HF) is characterized by sympathetic overactivity and enhanced circulating catecholamines (CAs), which significantly increase HF morbidity and mortality. We recently reported that adrenal G protein-coupled receptor kinase 2 (GRK2) is up-regulated in chronic HF, leading to enhanced CA release via desensitization/down-regulation of the chromaffin cell α_2-adrenergic receptors that normally inhibit CA secretion. We also showed that adrenal GRK2 inhibition decreases circulating CAs and improves cardiac inotropic reserve and function. Herein, we hypothesized that adrenal-targeted GRK2 gene deletion before the onset of HF might be beneficial by reducing sympathetic activation. To specifically delete GRK2 in the chromaffin cells of the adrenal gland, we crossed PNMTCre mice, expressing Cre recombinase under the chromaffin cell-specific phenylethanolamine *N*-methyltransferase (PNMT) gene promoter, with *floxed*GRK2 mice. After confirming a significant (~50%) reduction of adrenal GRK2 mRNA and protein levels, the PNMT-driven GRK2 knockout (KO) offspring underwent myocardial infarction (MI) to induce HF. At 4 weeks post-MI, plasma levels of both norepinephrine and epinephrine were reduced in PNMT-driven GRK2 KO, compared with control mice, suggesting markedly reduced post-MI sympathetic activation. This translated in PNMT-driven GRK2 KO mice into improved cardiac function and dimensions as well as amelioration of abnormal cardiac β-adrenergic receptor signaling at 4 weeks post-MI. Thus, adrenal-targeted GRK2 gene KO decreases circulating CAs, leading to improved cardiac function and β-adrenergic reserve in post-MI HF. GRK2 inhibition in the adrenal gland might represent a novel sympatholytic strategy that can aid in blocking HF progression.

Despite recent advances in prevention and management of heart disease, death due to chronic heart failure (HF)[3] continues to rise and new and innovative treatments are needed (1, 2). A salient feature of HF is elevated sympathetic nervous system (SNS) activity and outflow, reflected by increased circulating catecholamines (CAs). Initially an adaptive process to compensate for decreased function following cardiac injury through stimulation of β-adrenergic receptors (βARs), SNS activation becomes maladaptive, contributing significantly to disease morbidity and mortality (3–5). Levels of norepinephrine (NE) are associated with worsened prognosis in HF (6). Epinephrine (Epi) and, to a lesser extent, NE secretion from the adrenal medulla provides essentially all circulating CAs and is a fundamental component of SNS outflow (7, 8). Chronic CA elevation in the heart causes significant dysregulation of βARs that include a myriad of molecular abnormalities (9). Included is the up-regulation of G protein-coupled receptor kinase 2 (GRK2 or βARK1), which contributes significantly to βAR and ventricular dysfunction (4, 5).

α_2ARs play a crucial role in autocrine feedback inhibition of CA release from cardiac sympathetic nerve terminals and from the adrenal medulla. In the latter tissue, they reside in membranes of chromaffin cells, which are responsible for adrenal CA production (10, 11). The importance of α_2AR-mediated SNS activity regulation in cardiac disease has been well documented in a variety of knock-out (KO) mouse models (12–14), and in HF patients (15, 16). We recently reported that, in addition to myocardium, GRK2 is up-regulated in the adrenal gland in animal models of HF, leading to enhanced CA release via desensitization/down-regulation of the chromaffin cell α_2ARs (17). We also showed that adrenal GRK2 inhibition via adenoviral-mediated *in vivo* gene therapy using the βARKct (a GRK2 inhibitory peptide) (18) acutely decreases circulating CAs and improves cardiac inotropic reserve and function (17).

In the present study, we posited that adrenal-targeted GRK2 gene deletion, before the onset of HF, might be bene-

* This work was supported, in whole or in part, by National Institutes of Health Grants HL56205, HL61690, HL085503, and HL075443 (Project 2) and P01-HL091799 (to W. J. K.). This work was also supported by post-doctoral fellowships (to A. L. and G. R.) from the American Heart Association (Great Rivers Affiliate) and by Grant A75301 from the Commonwealth of Pennsylvania Dept. of Health.

[1] Supported by a Scientist Development Grant from the American Heart Association (AHA Grant 09SDG2010138, National Center). To whom correspondence should be addressed: Dept. of Pharmaceutical Sciences, Nova Southeastern University College of Pharmacy, 3200 S. University Dr., HPD (Terry) Bldg., Rm. 1338, Ft. Lauderdale, FL 33328. Tel.: 954-262-1338; Fax: 954-262-2278; E-mail: al806@nova.edu.

[2] Present address: Cardiology Division, Fondazione Salvatore Maugeri, Scientific Institute of Telese Terme, Telese Terme, Italy.

[3] The abbreviations used are: HF, heart failure; SNS, sympathetic nervous system; CA, catecholamine; βAR, β-adrenergic receptor; α_2AR, α_2-adrenergic receptor; NE, norepinephrine; Epi, epinephrine; GRK2, G protein-coupled receptor kinase 2; KO, knock-out; PNMT, phenylethanolamine *N*-methyltransferase; MI, myocardial infarction; WT, wild type; TH, tyrosine hydroxylase; BNP, brain natriuretic peptide; GAPDH, glyceraldehyde 3-phosphate dehydrogenase.

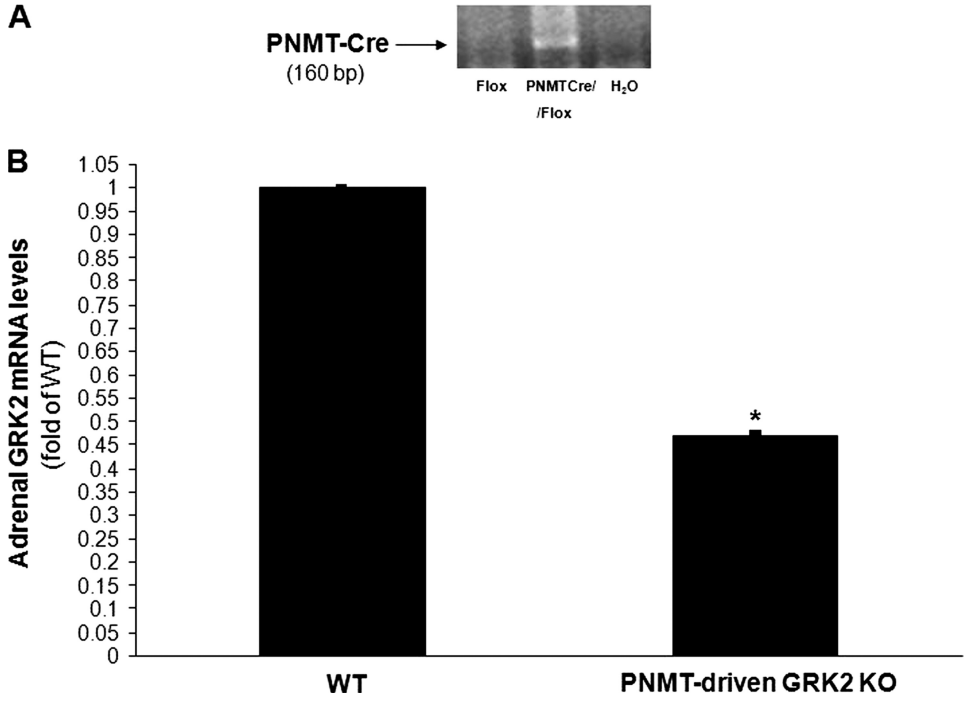

FIGURE 1. *A*, PCR screening in tail genomic DNA from PNMTCre/*Floxed*GRK2 (*PNMTCre/Flox*) or control *Floxed*GRK2 (*Flox*) mice for confirmation of PNMT locus insertion of the Cre transgene. An additional *lane* run without DNA (H_2O), thus serving as negative control for the assay is also shown. *B*, real-time PCR in total adrenal mRNA isolated from 2-month-old PNMT-driven GRK2 KO or control *Floxed*GRK2 (WT) mice for determination of total adrenal GRK2 mRNA levels (*, $p < 0.05$, $n = 6$ mice/litter).

ficial by reducing sympathetic activation. To specifically delete GRK2 in the chromaffin cells of the adrenal gland, we took advantage of the Cre/*lox*P technology (19) and crossed PNMTCre mice, expressing Cre recombinase under the gene promoter of the chromaffin cell-specific enzyme phenylethanolamine *N*-methyl transferase (PNMT) (20), with *floxed*GRK2$^{+/+}$ mice (21). To induce HF, resultant mice homozygous for the *floxed* allele (*i.e.* PNMTCre$^{+/-}$/*floxed*GRK2$^{+/+}$) and control mice with endogenous GRK2 expression underwent myocardial infarction (MI) and were studied at 4 weeks post-MI. Our data demonstrate that reduction of circulating CAs via adrenal-targeted GRK2 gene deletion can improve cardiac function and βAR signaling post-MI, and this sympatholysis is beneficial in HF.

EXPERIMENTAL PROCEDURES

Mouse Generation, PCR Screening, and Real-time PCR—Screening for the presence of the PNMT-Cre transgene was done in genomic tail DNA from transgenic mice by PCR using a specific primer mix, as described before (20). Real-time reverse transcription-PCR was carried out as described (17).

Western Blotting—Western blotting was performed in protein extracts of whole adrenal glands and hearts using appropriate specific antibodies, as described previously (17).

Surgical MI—All animal procedures and experiments were performed in accordance with the guidelines of the Institutional Animal Care and Use Committee of Thomas Jefferson University. MI was induced by high ligation of the left anterior descending coronary artery, as described previously (22).

Plasma and in Vitro CA Measurements—Plasma NE and epinephrine were determined with the BI-CAT EIA kit from ALPCO Diagnostics (Windham, NH), as described before (17).

Echocardiographic and Hemodynamic Measurements—Two-dimensional guided M-mode and Doppler echocardiography and closed chest cardiac catheterization were performed in mice as described (17, 22).

Chromaffin Cell Culture and in Vitro CA Secretion Assays—Chromaffin cells were isolated from adrenal glands excised from the mice and cultured as described previously (17). The purity of cultured chromaffin cells was assessed morphologically and by immunofluorescence and/or immunoblotting for endogenous expression of tyrosine hydroxylase; purity was over 90% in all experiments.

α_2AR Density Measurements—Plasma membranes from excised adrenal glands were prepared as described (17), and saturation binding was performed using the α_2AR-specific antagonist [^{3}H]rauwolscine. Data were analyzed by nonlinear regression analysis using Prism (GraphPad).

Cardiac βAR Density and cAMP Measurements—βAR density was measured in isolated cardiac plasma membranes using ^{125}I-CYP (iodocyanopindolol), as described before (23). Cardiac cAMP levels were measured with the BIOMOL Cyclic AMP PLUS EIA kit (Biomol, Plymouth Meeting, PA), as described (23).

Statistical Analysis—Data are summarized as mean ± S.E. Comparisons were made using *t* tests or analysis of variance as appropriate. A Bonferroni correction was applied to the probability values whenever multiple comparisons arose. Values of $p < 0.05$ were considered significant.

RESULTS

Generation of PNMT-driven GRK2 KO Mice—PNMT-driven GRK2 KO mice were generated by crossing the PNMT-Cre and the *floxed*GRK2$^{+/+}$ mouse lines and breeding the offspring to *floxed* allele homozygosity. All the mice used in the present study were heterozygous for the PNMT-Cre allele and homozygous for the *floxed*GRK2 allele (PNMTCre$^{+/-}$/floxGRK2$^{+/+}$). PCR screening in tail genomic DNA confirmed the presence of the PNMT-Cre allele in the offspring (Fig. 1*A*). GRK2 gene deletion induced by adrenal chromaffin cell expression of Cre recombinase led to a significant (53.1 ± 0.5%) reduction of total adrenal GRK2 mRNA levels in the PNMT-driven GRK2 KO mice compared with control wild-type (WT) *floxed*GRK2$^{+/+}$ mice (Fig. 1*B*). Of note, total adrenal mRNA levels of GRK3 and GRK5, the two most important of the other ubiquitously

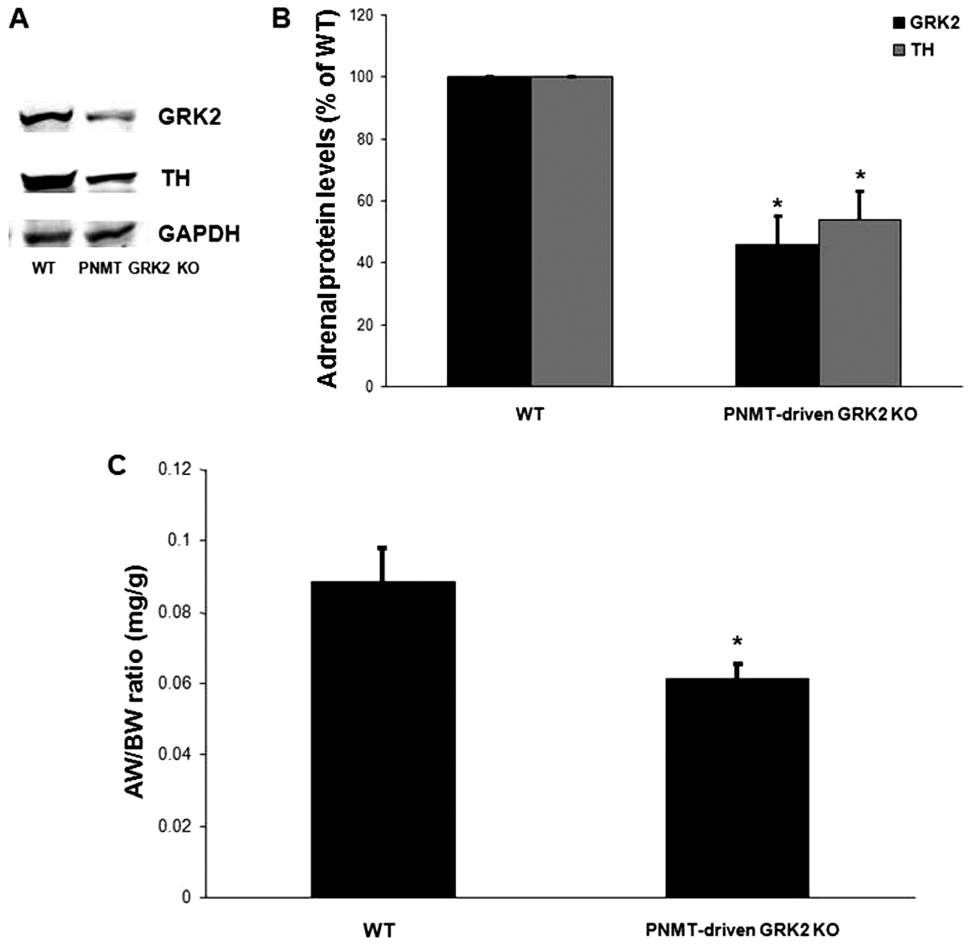

FIGURE 2. *A*, representative Western blots in total adrenal protein extracts from 2-month-old PNMT-driven GRK2 KO or control *Floxed*GRK2 (*WT*) mice for total adrenal GRK2 or tyrosine hydroxylase (*TH*) protein levels. Blots for the housekeeping protein glyceraldehyde 3-phosphate dehydrogenase (*GAPDH*), as loading control, are also shown. *B*, densitometric quantitation of the four independent experiments done in *A* using GAPDH levels as normalization control (*, $p < 0.05$, *versus* WT, $n = 4$ independent experiments performed in extracts from 6 adrenals pooled from 3 mice/litter each). *C*, adrenal weight-to-body weight ratios of these mice (see also Table 2) (*, $p = 0.023$, $n = 10$ mice/litter).

TABLE 1

Basic phenotypic characteristics of 2-month-old male WT and PNMT-driven GRK2 KO mice

	WT	PNMT-driven GRK2 KO
Heart weight	140 ± 5.0 mg	136 ± 4.0 mg
Adrenal weight	2.5 ± 0.2 mg	1.6 ± 0.3 mg[a]
Body weight	27.8 ± 0.9 g	26.9 ± 1.0 g
Liver weight	2.1 ± 0.2 g	2.2 ± 0.2 g
Lung weight	175 ± 13 mg	181 ± 11 mg
Kidney weight	630 ± 71 mg	645 ± 75 mg

[a] $p < 0.05$ *versus* WT, $n = 10$. Note: The basic cardiac functional parameters of these mice are presented in Table 2 (see columns for Sham/WT and Sham/KO of Table 2).

expressed GRKs (4), were unchanged (data not shown), confirming the specificity of this genetic deletion approach as well as the fact that it did not cause any compensatory changes in the levels of other adrenal GRKs when GRK2 was lost. Importantly, Western blotting of total adrenal protein extracts from PNMT-driven GRK2 KO and WT mice confirmed a significant loss (~50%) of GRK2 protein consistent with the loss of GRK2 gene expression in only the chromaffin cells (Fig. 2, *A* and *B*).

Adrenal Phenotypic Characterization of PNMT-driven GRK2 KO Mice—After confirming the success of GRK2 gene deletion in CA-producing chromaffin cells, we investigated the adrenal phenotype of PNMT-driven GRK2 KO mice. First, PNMT-driven GRK2 KO mice are viable, reproduce normally, and present without any significant abnormalities. Previously, we have found that, in HF, adrenal GRK2 up-regulation is accompanied by significant adrenal hypertrophy and elevated CA biosynthetic activity, as reflected by tyrosine hydroxylase (TH) up-regulation, the enzyme that catalyzes the rate-limiting step in CA biosynthesis (7, 8). Therefore, we measured adrenal size and TH expression in adult (2-month-old) PNMT-driven GRK2 KO and WT mice. We found that chromaffin cell GRK2 deletion leads to a significant decrease of adrenal size (Fig. 2*C* and Table 1). In addition, adrenal TH is down-regulated to a similar extent (~50% at the protein level) in 2-month-old PNMT-driven GRK2 KO mice compared with age-matched control WT mice (Fig. 2, *A* and *B*). A full outline of the overt phenotypic features of these mice can be found in Table 1. Taken together, these results suggest that chromaffin cell GRK2 deletion leads to attenuation of adrenal growth and CA biosynthetic activity during development.

Adrenal α_2AR Signaling Status in PNMT-driven GRK2 KO Mice—We also investigated the impact of chromaffin cell-targeted GRK2 deletion on the signaling status of the sympatho-inhibitory α_2ARs, which regulate CA secretion from these cells (8, 10). Saturation ligand binding in plasma membranes from the adrenal glands of PNMT-driven GRK2 KO mice revealed a significant up-regulation of α_2ARs compared with age-matched control WT mice (Fig. 3*A*). Consistent with this, *in vitro* CA secretion assays in chromaffin cells isolated and cultured from the adrenals of these mice showed that, in cells derived from PNMT-driven GRK2 KOs, the α_2AR agonist UK14304 is capable of producing a larger (maximal) inhibition of nicotine-induced CA secretion compared with WT mouse-derived chromaffin cells (Fig. 3*B*). Taken together, these experiments confirm that the absence of GRK2 from the chromaffin cells of PNMT-driven GRK2 KO mice leads to increases in both functional α_2AR number and α_2AR signaling/function in these cells, thus providing proof of concept for the generation of these mice.

Levels of Post-MI HF Sympathetic Activation in PNMT-driven GRK2 KO Mice—We have previously reported that adrenal GRK2 is an important regulator of adrenal CA secretion and hence of circulating CA levels, both in normal animals

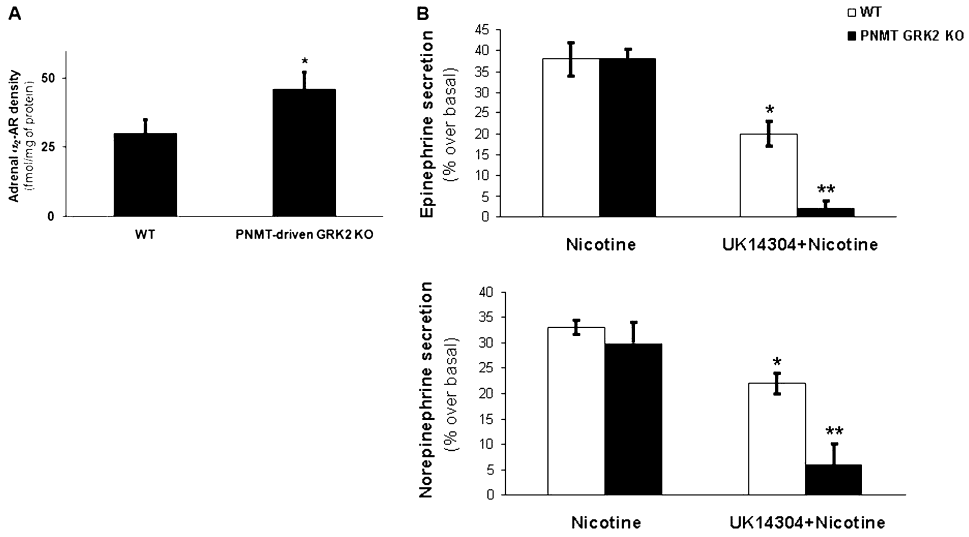

FIGURE 3. *A*, plasma membrane α_2AR density in the adrenal glands of 2-month-old PNMT-driven GRK2 KO or control *Floxed*GRK2 (*WT*) mice. Nonspecific binding was determined in the presence of 0.4 mM phentolamine (*, $p < 0.05$, *versus* WT, $n = 3$ independent experiments, performed with 8 adrenals pooled from 4 mice/litter each). Data are expressed as mean ± S.E. *B*, *in vitro* catecholamine secretion from chromaffin cells isolated from these mice after nicotine treatment, following pretreatment with vehicle (*Nicotine*) or with 10 μM UK14304 (*UK14304 + Nicotine*). UK14304 pretreatment alone had no effect (data not shown) (*, $p < 0.05$, *versus* WT/nicotine, **, $p < 0.05$, *versus* WT/UK14304 + nicotine, $n = 3$ independent experiments, performed with cells isolated from 10 adrenals pooled from 5 mice/litter each).

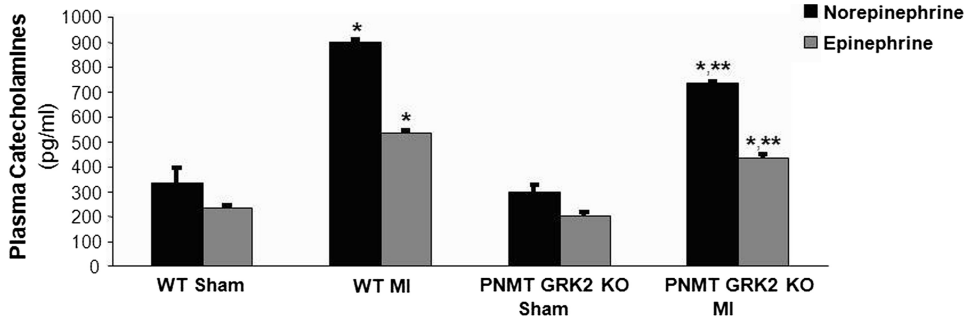

FIGURE 4. **Plasma circulating norepinephrine and epinephrine levels in normal, sham-operated (*Sham*) or in 4-week post-MI HF (*MI*) PNMT-driven GRK2 KO (*PNMT GRK2 KO*) and control *Floxed*GRK2 (*WT*) mice.** *, $p < 0.05$, *versus* Sham-either genotype; **, $p < 0.05$, *versus* WT MI, $n = 6$ mice/group.

and in HF (17, 24). Thus, we investigated the impact of GRK2 loss in chromaffin cells on circulating plasma CA levels. We measured CA levels in PNMT-driven GRK2 KO and WT mice under basal conditions (using Sham-operated mice) and also 4 weeks after surgically induced MI. Interestingly, plasma levels of both NE and Epi were similar between Sham WT and PNMT-driven GRK2 KO mice (Fig. 4). This is consistent with the reported finding that mono-allelic Cre insertion into the PNMT locus does not result in changes of the levels of either catecholamine (20). Indeed, plasma levels of both NE and Epi were similar between the control WT *floxed*GRK2$^{+/+}$ used in this study and PNMT-Cre$^{+/-}$ mice (data not shown). Following MI (4 weeks), we found that overall survival post-MI was similar in both groups of mice (data not shown), however, we found a significant difference in plasma CAs 4 weeks post-MI as both NE and Epi levels were significantly lower in PNMT-driven GRK2 KO mice compared with WT mice (Fig. 4). This result strongly suggests that PNMT-driven GRK2 deletion results in significant attenuation of post-MI sympathetic activation/increased outflow.

In Vivo Cardiac Function 4 Weeks after MI—We next investigated the impact of reduced post-MI circulating CA levels in PNMT-driven GRK2 KO mice on the development of cardiac dysfunction. As shown in Fig. 5*A*, cardiac ejection fraction is significantly increased in KO mice compared with WT mice (>10% improvement) at 4 weeks post-MI, whereas both groups of sham-operated animals exhibited similar ejection fraction values. Further, post-MI left ventricular (LV) remodeling was slightly but significantly attenuated in KO mice compared with WT mice as indicated by the reduction of LV end-diastolic diameter (Fig. 5*B*). Additionally, *in vivo* cardiac catheterization of these mice at 4 weeks post-MI revealed markedly decreased basal and isoproterenol-induced cardiac contractility in both groups compared with sham animals (Fig. 5*C*). Importantly, although basal $+dP/dt_{max}$ responses were similar between PNMT-driven GRK2 KO and WT mice post-MI, PNMT-driven GRK2 KO mice had significantly improved responsiveness to isoproterenol compared with post-MI WT mice (Fig. 5*C*).

Of note, LV infarct size was similar between the two groups at 24 h post-MI (Fig. 6), and at 4 weeks post-MI (data not shown), indicating that this improvement in cardiac function observed in PNMT-driven GRK2 KOs at 4 weeks post-MI was not due to differences in initial myocardial damage caused by the coronary artery ligation or in viable/functional myocardial mass between the two groups. Table 2 provides a complete outline of the *in vivo* echocardiographic and hemodynamic parameters of the sham and 4-week post-MI HF mice within both groups. Taken together, the above physiological data suggest that cardiac function and β-adrenergic-stimulated inotropic reserve at 4 weeks post-MI are significantly improved by the reduction in circulating CA levels due to the chromaffin cell-targeted GRK2 deletion. In other words, there is less cardiac dysfunction 4 weeks post-MI when CA levels are decreased due to a loss of adrenal GRK2 expression.

Myocardial β-Adrenergic Signaling Status at 4 Weeks Post-MI—We also examined whether the observed improvement in cardiac function of post-MI PNMT-driven GRK2 KO mice translated into positive alteration of cardiac βAR signaling at the molecular level, because lower sympathetic overdrive during HF progression could mean less βAR desensitization and down-regulation. Accordingly, hearts from both sham-op-

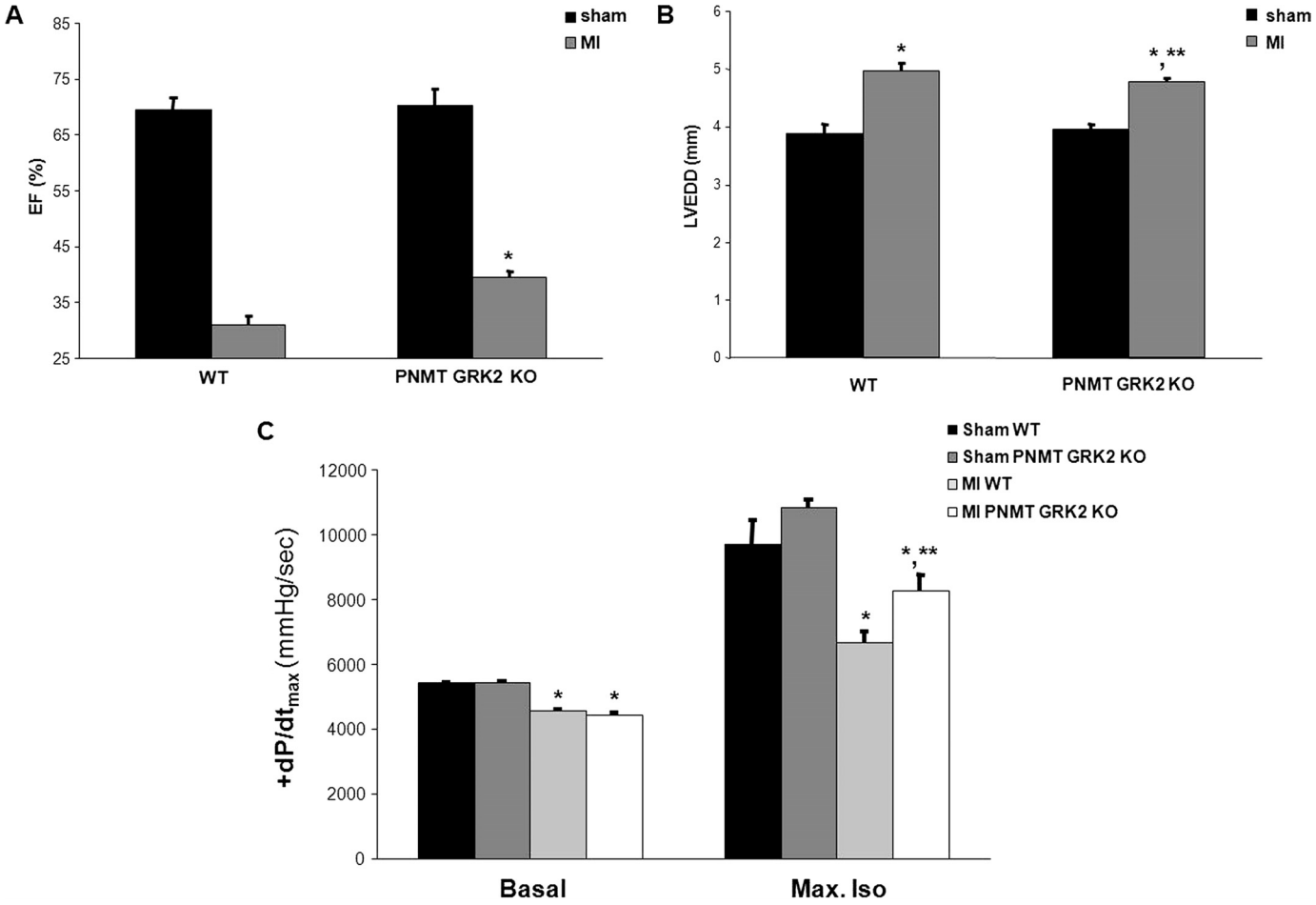

FIGURE 5. *A*, ejection fraction (*EF %*) of sham-operated (*sham*) or of 4-week post-MI HF (*MI*) PNMT-driven GRK2 KO (*PNMT GRK2 KO*) and control *Floxed*GRK2 (*WT*) mice (*, $p = 0.005$, *versus* WT MI, $n = 10$ mice/group). *B*, LV end diastolic diameter (*LVEDD*) of these mice (*, $p < 0.05$, *versus* sham; **, $p < 0.05$, *versus* WT MI, $n = 10$ mice/group). *C*, basal and maximal dose of isoproterenol (*Max. Iso*)-stimulated + dP/dt_{max} responses of these mice (*, $p < 0.05$, *versus* sham; **, $p < 0.05$, *versus* Max. Iso/MI WT, $n = 7$ mice/group).

erated and HF mouse lines were excised at 4 weeks post-MI, and total βAR density in plasma membranes isolated from these hearts was measured. As expected, HF caused a marked cardiac βAR down-regulation in both mouse lines at 4 weeks post-MI, compared with healthy sham animals (Fig. 7*A*). However, in post-MI failing KO hearts this βAR down-regulation was significantly attenuated compared with control WT hearts (Fig. 7*A*). In addition, we also measured total steady-state cAMP levels in these hearts. cAMP is a second messenger activated by myocardial βARs crucial for their pro-contractile signaling (3, 4). As shown in Fig. 7*B*, myocardial cAMP levels in HF control WT hearts were significantly reduced compared with sham hearts, consistent with impaired βAR signaling in HF. Cardiac cAMP levels of HF PNMT-driven GRK2 KO mice however were essentially restored to the levels of sham hearts (Fig. 7*B*), indicating a marked amelioration of cardiac βAR signaling in adrenal-targeted GRK2-depleted mice at 4 weeks post-MI. It is important to note that the levels of cAMP in PNMT-driven GRK2 KO hearts were not elevated above sham (non-failing) heart levels and that levels appear to be normalized (Fig. 7*B*).

Finally, we measured myocardial GRK2 levels and found that GRK2 was significantly increased in HF control WT hearts, again as expected (Fig. 7, *C* and *D*). Interestingly, GRK2 levels in PNMT-driven GRK2 KO hearts, albeit no different from WT hearts in sham healthy animals, were markedly reduced at 4 weeks post-MI compared with WT hearts at the same time point, to even below the levels of sham hearts (Fig. 7, *C* and *D*), suggesting a complete prevention and/or reversal of the contractility-suppressive cardiac GRK2 up-regulation in failing PNMT-driven GRK2 KO hearts. Taken together, these results indicate that the reduction of catecholaminergic stimulation of the failing heart by the adrenal-specific GRK2 deletion significantly ameliorates myocardial βAR number, signaling, and function, which probably underlies, in turn, the improvement in cardiac function.

Cardiac Remodeling and Functional Biomarkers at 4 Weeks Post-MI—To further analyze morphological and molecular aspects of adverse cardiac remodeling, we also assessed mRNA expression levels of specific genes known to play important roles in HF pathogenesis. The heart weight-to-body weight ratio was significantly increased in control WT mice at 4 weeks post-MI compared with the sham groups consistent with a HF phenotype, while cardiac mass was significantly decreased in PNMT-driven GRK2 KO mice 4 weeks after MI (Table 2). For molecular LV remodeling and hypertrophy status characterization, we measured the mRNA levels of collagen 1, atrial natri-

uretic factor, and transforming growth factor-β1 in the LV of all groups via reverse transcription-PCR. Consistent with the echocardiographic data presented above (Fig. 5), collagen 1, atrial natriuretic factor, and transforming growth factor-β1 mRNA levels were markedly increased in control WT hearts at 4 weeks post-MI, as expected, and levels of these detrimental cardiac markers were significantly reduced in PNMT-driven GRK2 KO hearts over the same post-MI time period (Fig. 8, *A–C*). These results demonstrate that the reduction of cardiac sympathetic activation by the adrenal-specific GRK2 deletion results in significant attenuation of post-MI HF-related remodeling. Finally, mRNA levels of brain natriuretic peptide (BNP), a fetal gene marker of cardiac hypertrophy, HF, and volume overload, were measured. Levels of BNP were again markedly elevated in control WT hearts at 4 weeks post-MI as expected, whereas KO hearts showed significantly lowered BNP expression (Fig. 8*D*). This favorable change in BNP levels is entirely consistent with the echocardiographic and hemodynamic analysis results presented above (Fig. 5 and Table 2). Of note, the adrenal hypertrophy present in WT mice after MI, as expected (17), appears significantly attenuated in PNMT-driven GRK2 KO mice at 4 weeks post-MI, as well (Table 2).

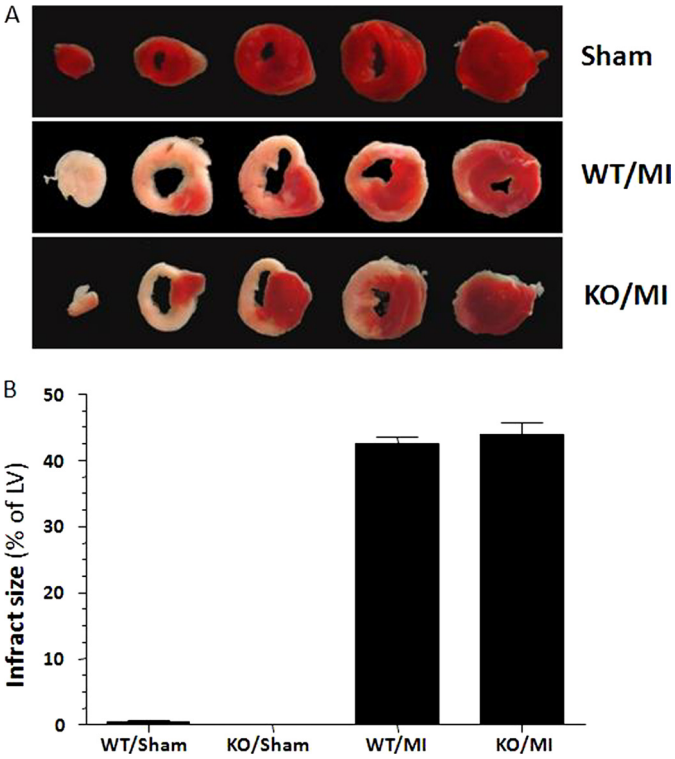

FIGURE 6. **Infarct size in PNMT-driven GRK2 KO (*KO*) and WT mice at 24 h post-MI.** Sham hearts are also shown as negative controls. *A*, representative triphenyltetrazolium chloride-stained cardiac cross-sections. *B*, average LV infarct size ($n = 5$ for each group). No significant difference between the MI groups was observed ($p = 0.05$).

DISCUSSION

In previous studies, we documented a crucial role for adrenal GRK2 in regulation of cardiac sympathetic stimulation, both under normal conditions and in the context of chronic HF (17, 24; reviewed in Ref. 11). In the present study, we sought to investigate whether suppression of adrenal GRK2 before the onset of HF can confer any benefit in progressing post-MI HF by reducing cardiac sympathetic burden. To this end, we developed a new transgenic mouse model having the GRK2 gene specifically deleted in the chromaffin cells of the adrenal medulla (PNMT-driven GRK2 KO), by utilizing the well established Cre/*lox*P technology (19), and we induced chronic HF by surgical MI in these mice. Our findings show that adrenal-restricted GRK2 deletion indeed leads to a significant reduction of circulating CAs *in vivo* in post-MI HF, thus proving the con-

TABLE 2

Cardiac functional parameters in sham and post-MI WT and PNMT-driven GRK2 KO mice

Echocardiographic and hemodynamic analysis data from 3-month-old sham-operated (Sham) or post-MI WT and PNMT-driven GRK2 KO mice on day 28 post-MI. Analysis of variance with the Bonferroni test was performed among all groups. Data are presented as mean ± S.E. $+dP/dt_{max}$, maximal first derivative of LV pressure rise; $-dP/dt_{min}$, minimal first derivative of LV pressure fall; HR, heart rate; LVESP, LV end systolic pressure; LVEDP, LV end diastolic pressure; LVIDd, LV inner diameter during diastole; LVIDs, LV inner diameter during systole; FS, fractional shortening; EF, ejection fraction; PWTd, posterior wall thickness in diastole; HW/BW, heart weight-to-body weight ratio; AW/BW, adrenal weight-to-body weight ratio; and LV, left ventricular.

	Sham/WT	Sham/KO	Post-MI/WT	Post-MI/KO
LVIDs (mm)	2.34 ± 0.08	2.32 ± 0.11	4.39 ± 0.12[a]	3.31 ± 0.21[a,b]
LVIDd (mm)	3.88 ± 0.15	3.96 ± 0.08	4.99 ± 0.12[a]	4.69 ± 0.06[a,b]
FS (%)	38.52 ± 0.14	39.25 ± 2.39	13.77 ± 1.13[a]	20.11 ± 0.35[a,b]
EF (%)	69.6 ± 1.97	70.12 ± 3.02	30.90 ± 1.65[a]	41.17 ± 0.97[a,b]
PWTd (mm)	0.95 ± 0.05	1.00 ± 0.02	1.28 ± 0.01[a]	1.11 ± 0.04[a,b]
Basal hemodynamic measurements				
HR (min^{-1})	468.2 ± 2.9	477.6 ± 11.5	457.6 ± 12.5	456.3 ± 8.7
$+dP/dt_{max}$ (mmHg/s)	5,430 ± 29	5,432 ± 49	4,552 ± 63[a]	4,448 ± 75[a]
$-dP/dt_{min}$ (mmHg/s)	−5,159 ± 206	−5,041 ± 101	−4,379 ± 104[a]	−4,298 ± 57[a]
LVESP (mmHg)	98.4 ± 1.1	98.8 ± 1.86	83.43 ± 4.4[a]	86.14 ± 1.8[a]
LVEDP (mmHg)	3.8 ± 0.4	4.0 ± 0.4	11.2 ± 0.8[a]	10.7 ± 1.4[a]
Hemodynamic measurements after maximal isoproterenol (333 ng/kg BW)				
HR (min^{-1})	576 ± 17.2	581 ± 7.2	578 ± 13.3	582 ± 7.1
$+dP/dt_{max}$ (mmHg/s)	9,717 ± 740	10,451 ± 230	6,689 ± 328[a]	8,273 ± 489[a,b]
$-dP/dt_{min}$ (mmHg/s)	−8,456 ± 438	−8,380 ± 255	−6,557 ± 392[a]	−6,647 ± 318[a]
LVESP (mmHg)	101 ± 2.3	101 ± 1.8	86 ± 3.1[a]	89 ± 3.4[a]
LVEDP (mmHg)	4.8 ± 1.4	4.6 ± 0.6	12.4 ± 0.9[a]	12.25 ± 0.5[a]
Phenotypic data				
HW/BW (mg/g)	5.03 ± 0.18	5.06 ± 0.13	9.8 ± 0.32[a]	8.2 ± 0.09[a,b]
AW/BW (mg/g)	0.09 ± 0.01	0.06 ± 0.01[c]	0.38 ± 0.06[a]	0.19 ± 0.03[a,b]

[a] $p < 0.05$ *versus* the sham line.
[b] $p < 0.05$ *versus* post-MI/WT.
[c] $p < 0.05$ *versus* Sham/WT, $n = 10$ mice/group for echo, HW/BW, and AW/BW measurements, $n = 7$ mice/group for hemodynamic measurements.

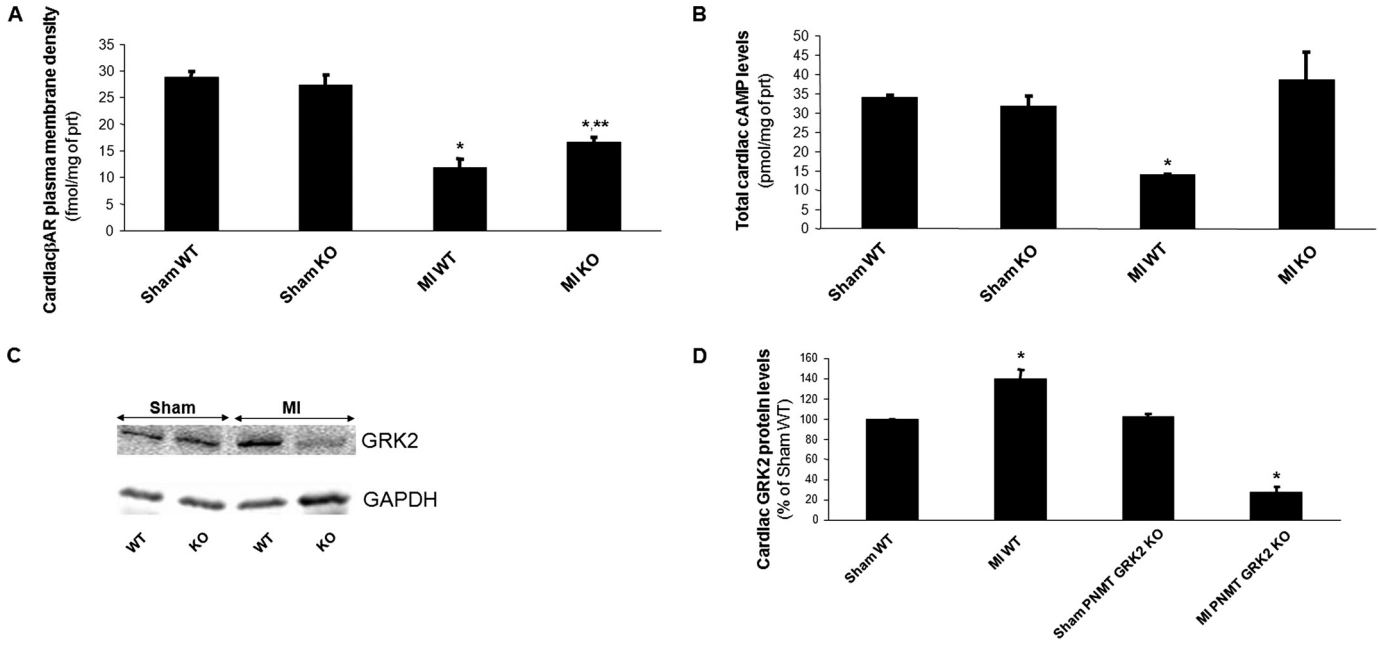

FIGURE 7. *A*, βAR density in cardiac plasma membranes of sham-operated (*sham*) or of 4-week post-MI HF (*MI*) PNMT-driven GRK2 KO (*KO*) and control WT mice. *, $p < 0.01$, *versus* either Sham (**, $p < 0.05$ *versus* MI WT, $n = 6$ hearts/group). *B*, steady-state total cAMP levels in cardiac homogenates purified from hearts of these mice (*, $p < 0.05$ *versus* all other groups, $n = 6$ hearts/group). *C*, representative Western blots in total cardiac protein extracts from these mice for cardiac GRK2 protein levels. Blots for the housekeeping protein glyceraldehyde 3-phosphate dehydrogenase (*GAPDH*), as loading control, are also shown. *D*, densitometric quantitation of the blots done in *C*, using GAPDH levels as normalization control (*, $p < 0.05$, *versus* respective Sham, $n = 6$ hearts/group).

cept of the transgenic animal approach employed, and, importantly, this resultant reduction of both circulating CAs (NE and Epi) appears indeed to impede the deterioration of cardiac function and βAR signaling, which are hallmarks of the post-MI chronic HF progression.

Previously, GRK2 was found, by tightly regulating the activity and function of the sympatho-inhibitory α_2ARs of the adrenal gland and of the central SNS, to be a key regulator of the CA levels present at the heart at any given time and, hence, of the levels of cardiac catecholaminergic stimulation, which is an important factor affecting morbidity and mortality in HF (6, 9). Moreover, we have shown that adrenal GRK2 inhibition via adenoviral-mediated *in vivo* gene therapy acutely decreases circulating CAs and improves cardiac inotropic reserve and function in rats with already established HF (10 weeks post-MI) (17). With the data from the current study, it is now even clearer that lowered GRK2 expression and activity in the adrenal gland can have a significant beneficial impact on the injured heart by imparting a sympatholytic effect on CA secretion from the adrenal medulla.

Importantly, the PNMT-driven GRK2 KO mice appear viable and normal and present no gross phenotypic abnormalities. Interestingly, with regard to their adrenal phenotype, they appear to have significantly reduced CA biosynthetic activity, as reflected by the down-regulation of TH present in their adrenals. In addition, the size of their adrenals is reduced compared with WT animals at 2 months of age (Table 1), and, intriguingly, they also display significantly attenuated adrenal hypertrophy at 4 weeks post-MI (Table 2). Thus, adrenal GRK2 seems to be an important trophic factor for the adrenal gland in health, but also a major driving force behind adrenal hypertrophy and hyperfunctioning in HF. These findings are also consistent with the up-regulation of adrenal TH and the enhanced adrenal hypertrophy observed in HF rats, where adrenal GRK2 is also up-regulated, and also with the reduction of adrenal TH levels of HF rats observed when adrenal GRK2 is inhibited *in vivo* (17). In addition, GRK2 emerges as a critical regulator of adrenal CA biosynthetic function in general, with its activity driving the organ toward increased production of CAs. The mechanisms for this are not clear at the moment. It could very well be an indirect mechanism, *i.e.* increased GRK2 leads to enhanced CA secretion, which in turn forces the adrenal medulla to produce more CAs to meet the growing demand, but GRK2 might also be more directly involved in adrenal CA biosynthesis, *e.g.* via regulation of specific biosynthetic enzymes. In any case, the mechanisms of this relationship of GRK2 with CA biosynthetic function in the adrenal gland will be of great interest to study and will be the focus of future studies.

Perhaps the most important finding of the present study is that adrenal-targeted GRK2 deletion caused a substantial reduction in circulating CAs post-MI, although it did not affect CA levels in normal, sham-operated mice. This finding confirms that the genetic perturbations employed to create this PNMT-driven GRK2 KO line did not have any nonspecific, non-adrenal GRK2-related effects on circulating CAs. More importantly, it also strongly suggests that adrenal GRK2 is absolutely crucial for the elevation of CA levels in post-MI HF, and thus, inhibition/suppression of adrenal GRK2 activity early on after the occurrence of an MI can have a powerful sympatholytic effect, which is very beneficial in the post-MI HF setting (9, 25).

Admittedly, the reduction in circulating CAs conferred by adrenal-specific GRK2 deletion in the present study appears relatively small, perhaps smaller than might have been ex-

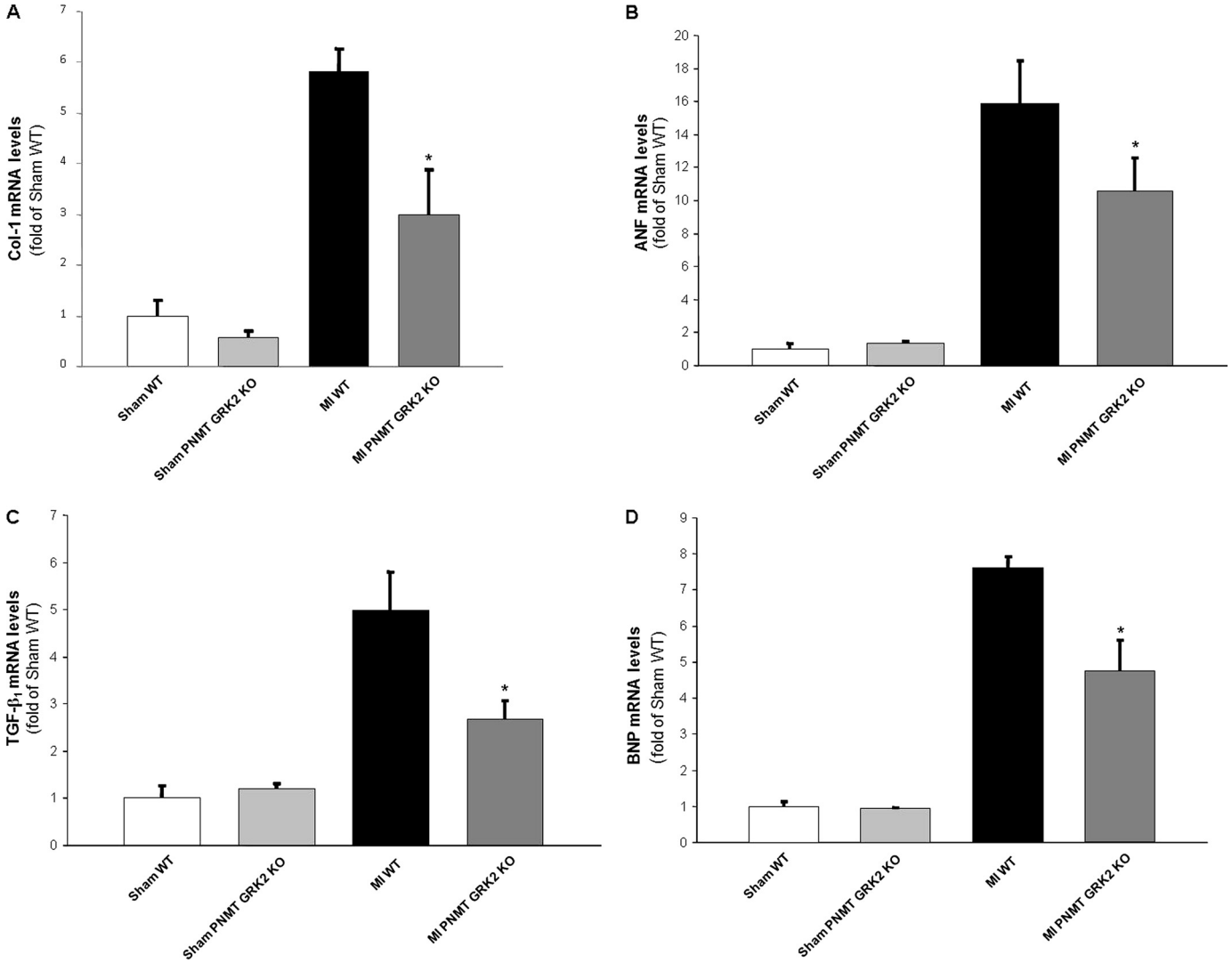

FIGURE 8. **Heart mRNA levels of collagen I (*A*), atrial natriuretic factor (*B*), transforming growth factor β1 (*C*), and brain natriuretic peptide (*D*) in all experimental groups at 4 weeks post-MI.** All values were standardized to amplified 28 S rRNA. Data are presented as mean ± S.E. and plotted as fold of sham WT values (*, $p < 0.05$, *versus* MI WT, $n = 6$ hearts/group).

pected, bringing circulating CA levels nowhere near the normal (sham) values. However, this can be explained by the fact that, in the PNMT-driven GRK2 KO model described here, GRK2 is deleted only in Epi-producing cells and tissues, not in every sympathetic tissue in the body (20). Therefore, sympathetic neurons can still produce and release NE normally. On the other hand, NE can still normally stimulate βARs present in central (or other) adrenergic/sympathetic neurons, which facilitate NE and/or Epi release (26); thus, even Epi might not be substantially reduced by the GRK2 deletion in adrenal chromaffin cells. Therefore, when all these parameters are taken into account, the unchanged (with respect to wild type) CA levels in normal (sham) PNMT-driven GRK2 KO mice and the relatively small CA level reductions in these mice observed post-MI are not all that surprising. Nevertheless, even slight reductions in the catecholaminergic burden of the failing heart can have profound beneficial effects on cardiac function and overall clinical status of the HF patient (27). In fact, excessive plasma CA reduction has been postulated to actually be deleterious rather than beneficial in HF patients (27, 28). Thus, it is absolutely plausible that the reductions in circulating CAs we observed in the PNMT-driven GRK2 KO mice can significantly impact cardiac function and βAR signaling post-MI in a beneficial manner.

The final interesting finding of the present study is the observed down-regulation of GRK2 in the failing hearts of PNMT-driven GRK2 KO mice. Because myocardial GRK2 critically regulates cardiac βAR signaling and function and hence cardiac performance and its up-regulation post-MI is a major contributor to the functional worsening of the failing heart (3, 4, 5, 23), this finding is reflective of the improved cardiac βAR signaling and function induced by CA reduction in the HF PNMT-driven GRK2 KO mice. However, it additionally suggests a close dynamic regulation of myocardial GRK2 activity by the levels of cardiac catecholaminergic activation (23, 29), which in turn are tightly regulated by GRK2 activity in the adrenal glands and in the central SNS (11, 17). Thus, the findings of the present study reinforce the notion that GRK2 is a key molecule in fine-tuning cardiac function, both basally and after sympathetic stimulation, and in particular in circumstances

where this function is severely compromised, such as in the chronic HF setting (11).

Overall, the present study reports that adrenal-targeted GRK2 gene deletion helps halt progression of cardiac contractile dysfunction and adverse remodeling and restores the abnormalities of cardiac βAR signaling in post-MI chronic HF by significantly reducing circulating catecholamine levels after cardiac injury, which are extremely toxic for the failing heart (6, 25). Of note, the beneficial effects of adrenal-specific GRK2 deletion also include down-regulation of cardiac GRK2, an important indicator of cardiac dysfunction in HF, and are evident even without a dramatic reduction in CA levels, which could be detrimental for cardiac hemodynamic support of the circulation and incompatible with life (27, 28). Thus, reduction of sympathetic activity/outflow via adrenal GRK2 inhibition as early as possible in the course of post-MI HF progression emerges as an attractive therapeutic strategy in the management of LV dysfunction.

REFERENCES

1. Thomas, S., and Rich, M. W. (2007) *Heart Fail. Clin.* **3,** 381–387
2. Kaye, D. M., and Krum, H. (2007) *Nat. Rev. Drug Disc.* **6,** 127–139
3. Port, J. D., and Bristow, M. R. (2001) *J. Mol. Cell Cardiol.* **33,** 887–905
4. Rockman, H. A., Koch, W. J., and Lefkowitz, R. J. (2002) *Nature* **415,** 206–212
5. Tilley, D. G., and Rockman, H. A. (2006) *Exp. Rev. Cardiovasc. Ther.* **4,** 417–432
6. Cohn, J. N., Levine, T. B., Olivari, M. T., Garberg, V., Lura, D., Francis, G. S., Simon, A. B., and Rector, T. (1984) *N. Engl. J. Med.* **311,** 819–823
7. Hoffman, B. B., and Taylor, P. (2001) *Goodman & Gilman's: The Pharmacological Basis of Therapeutics,* 10th Ed., McGraw-Hill, New York, NY
8. Young, J. B., and Landsberg, L. (1998) *Williams Textbook of Endocrinology*, 9th Ed., Saunders, Philadelphia, PA
9. Mudd, J. O., and Kass, D. A. (2008) *Nature* **451,** 919–928
10. Brede, M., Nagy, G., Philipp, M., Sorensen, J. B., Lohse, M. J., and Hein, L. (2003) *Mol. Endocrinol.* **17,** 1640–1646
11. Lymperopoulos, A., Rengo, G., and Koch, W. J. (2007) *Trends Mol. Med.* **13,** 503–511
12. Hein, L., Altman, J. D., and Kobilka, B. K. (1999) *Nature* **402,** 181–184
13. Brede, M., Wiesmann, F., Jahns, R., Hadamek, K., Arnolt, C., Neubauer, S., Lohse, M. J., and Hein, L. (2002) *Circulation* **106,** 2491–2496
14. Brum, P. C., Kosek, J., Patterson, A., Bernstein, D., and Kobilka, B. (2002) *Am. J. Physiol. Heart Circ. Physiol.* **283,** H1838–H1845
15. Small, K. M., Wagoner, L. E., Levin, A. M., Kardia, S. L., and Liggett, S. B. (2002) *N. Engl. J. Med.* **347,** 1135–1142
16. Small, K. M., McGraw, D. W., and Liggett, S. B. (2003) *Annu. Rev. Pharmacol. Toxicol.* **43,** 381–411
17. Lymperopoulos, A., Rengo, G., Funakoshi, H., Eckhart, A. D., and Koch, W. J. (2007) *Nat. Med.* **13,** 315–323
18. Koch, W. J., Rockman, H. A., Samama, P., Hamilton, R. A., Bond, R. A., Milano, C. A., and Lefkowitz, R. J. (1995) *Science* **268,** 1350–1353
19. Wamhoff, B. R., Sinha, S., and Owens, G. K. (2007) *Handb. Exp. Pharmacol.* **178,** 441–468
20. Ebert, S. N., Rong, Q., Boe, S., Thompson, R. P., Grinberg, A., and Pfeifer, K. (2004) *Dev. Dyn.* **231,** 849–858
21. Matkovich, S. J., Diwan, A., Klanke, J. L., Hammer, D. J., Marreez, Y., Odley, A. M., Brunskill, E. W., Koch, W. J., Schwartz, R. J., and Dorn, G. W., 2nd (2006) *Circ. Res.* **99,** 996–1003
22. Raake, P. W., Vinge, L. E., Gao, E., Boucher, M., Rengo, G., Chen, X., DeGeorge, B. R., Jr., Matkovich, S., Houser, S. R., Most, P., Eckhart, A. D., Dorn, G. W., 2nd, and Koch, W. J. (2008) *Circ. Res.* **103,** 413–422
23. Rengo, G., Lymperopoulos, A., Zincarelli, C., Donniacuo, M., Soltys, S., Rabinowitz, J. E., and Koch, W. J. (2009) *Circulation* **119,** 89–98
24. Lymperopoulos, A., Rengo, G., Zincarelli, C., Soltys, S., and Koch, W. J. (2008) *Mol. Ther.* **16,** 302–307
25. Floras, J. S. (2002) *Circulation* **105,** 1753–1755
26. Eisenhofer, G., Kopin, I. J., and Goldstein, D. S. (2004) *Pharmacol. Rev.* **56,** 331–349
27. Liggett, S. B., Mialet-Perez, J., Thaneemit-Chen, S., Weber, S. A., Greene, S. M., Hodne, D., Nelson, B., Morrison, J., Domanski, M. J., Wagoner, L. E., Abraham, W. T., Anderson, J. L., Carlquist, J. F., Krause-Steinrauf, H. J., Lazzeroni, L. C., Port, J. D., Lavori, P. W., and Bristow, M. R. (2006) *Proc. Natl. Acad. Sci. U.S.A.* **103,** 11288–11293
28. Bristow, M. R., Krause-Steinrauf, H., Nuzzo, R., Liang, C. S., Lindenfeld, J., Lowes, B. D., Hattler, B., Abraham, W. T., Olson, L., Krueger, S., Thaneemit-Chen, S., Hare, J. M., Loeb, H. S., Domanski, M. J., Eichhorn, E. J., Zelis, R., and Lavori, P. (2004) *Circulation* **110,** 1437–1442
29. Iaccarino, G., Tomhave, E. D., Lefkowitz, R. J., and Koch, W. J. (1998) *Circulation* **98,** 1783–1789